JVI Journals.ASM.org

SAMD9 Is an Innate Antiviral Host Factor with Stress Response Properties That Can Be Antagonized by Poxviruses

Jia Liu,[a,b] Grant McFadden[c]

Department of Microbiology and Immunology[a] and Center for Microbial Pathogenesis and Host Inflammatory Response,[b] University of Arkansas for Medical Sciences (UAMS), Little Rock, Arkansas, USA; Department of Molecular Genetics and Microbiology, University of Florida College of Medicine, Gainesville, Florida, USA[c]

We show that SAMD9 is an innate host antiviral stress response element that participates in the formation of antiviral granules. Poxviruses, myxoma virus and vaccinia virus specifically, utilize a virus-encoded host range factor(s), such as a member of the C7L superfamily, to antagonize SAMD9 to prevent granule formation in a eukaryotic initiation factor 2α (eIF2α)-independent manner. When SAMD9 is stimulated due to failure of the viral antagonism during infection, the resulting antiviral granules exhibit properties different from those of the canonical stress granules.

Poxviruses are enveloped large double-stranded DNA (dsDNA) viruses that replicate exclusively in the cytoplasm. Numbers of immunoregulatory factors are encoded in the poxvirus genome to antagonize multiple host defense pathways at all levels. We previously showed that a targeted knockout of M062R, an essential host range factor of the C7L superfamily in the myxoma virus (MYXV) genome, led to a profound defect of viral replication in cells from all species tested, including human, rabbit, and primate cells (1). Viral M062 antagonizes cellular SAMD9 during viral infection through direct protein-protein interactions, and knocking down the expression of SAMD9 in human cells lifts the block of late gene expression from MYXV-M062R-null infection (1). To investigate the antiviral functions of SAMD9, we examined the cellular localization of this host protein during permissive wild-type and nonpermissive MYXV-M062R-null infection by immunofluorescence (IF) staining. We observed that, during MYXV-M062R-null infection, SAMD9 formed a granule structure in the cytoplasm. The accumulation of concentrated SAMD9 was detected as early as 7 h postinfection (p.i.). By 18 h p.i., 91.0% (±6.2% standard deviation [SD]) of infected cells showed SAMD9 granules which were then mostly concentrated near the viral factories (Fig. 1A). During permissive infection by wild-type MYXV that expressed M062 protein, SAMD9 was observed to become distributed throughout the cells, which was also distinct from the exclusive cytoplasmic localization of SAMD9 in uninfected cells. We further investigated the SAMD9 granules and found that they are not conventional stress granules (SGs), as they cannot be dispersed by cycloheximide treatment (not shown) in a manner similar to that seen with the antiviral granules previously described, which form after infection with E3L-knockout vaccinia virus (VACV) (2). On the other hand, several hallmark markers of SGs, such as rasGTPase-activating protein-binding protein 1 (G3BP1) (3) (Fig. 1), T-cell intracellular antigen 1-related protein (TIAR) (4), USP10 (5), and key translation initiation factors such as eukaryotic initiation factor 4G (eIF4G) (6) (Fig. 1B), were readily detected surrounding the viral factories colocalized with the SAMD9 granules in infection by MYXV-M062-null. However, in addition to the SAMD9 granules that overlap G3BP1 staining, SAMD9 staining can be detected outside the viral factories. The polyclonal SAMD9 antibody used in this study recognizes the N terminus of SAMD9; during the extensive posttranslational processing and/or cleavage in the cells, the N terminus of SAMD9 is mostly retained (not shown). Because SAMD9 full-length protein was shown to be the target of M062 (1), we reasoned that the presence of full-length SAMD9 is the force driving formation of the granule structure. Thus, the extensively processed products from full-length SAMD9 may explain the IF staining pattern that localizes in the region other than the granule structure. There is another difference from the results seen with canonical SGs: eIF4G staining did not exclusively colocalize with G3BP1 (Fig. 1B).

We then examined the behavior of the SAMD9 response following infection with E3L-knockout VACV (2). In addition, because MYXV-M062R is a functional homolog of VACV C7L, an orthologue of the poxvirus C7L superfamily (7, 8), we also investigated the relevance of the SAMD9 response to the function of C7L and its complementary viral factor, K1L. We constructed targeted E3L knockout VACV (VACV-E3LKO-$_{L}$tdTr), C7L and K1L double-knockout VACV (VACV-C7LK1L-DKO), and corresponding single-knockout viruses (VACV-C7LKO-$_{E/L}$GFP and VACV-K1LKO-$_{L}$tdTr) using an early/late green fluorescent protein ($_{E/L}$GFP) (1) or late tdTomato red ($_{L}$tdTr) (9) expression cassette to replace the respective specific genes. All constructed knockout VACVs showed consistent phenotypes as previously reported (2, 8, 10). At 5 h p.i., wild-type VACV (VACV-$_{E/L}$GFP/$_{L}$tdTr) (11) (Fig. 2A), VACV-C7LKO-$_{E/L}$GFP (not shown), or K1LKO-$_{L}$tdTr (Fig. 2A) infections did not stimulate the formation of SAMD9 granules. However, in VACV-E3LKO-$_{L}$tdTr and VACV-C7LK1L-DKO infection, SAMD9 nucleated to form granules at rates of 92.1% (±8.4% of SD) and 91.8% (±8.3% of SD), respectively. Specifically, G3BP1 and viral factories in VACV-E3LKO-$_{L}$tdTr-infected and VACV-C7LK1L-DKO-infected cells

Received 12 August 2014 **Accepted** 17 November 2014

Accepted manuscript posted online 26 November 2014

Citation Liu J, McFadden G. 2015. SAMD9 is an innate antiviral host factor with stress response properties that can be antagonized by poxviruses. J Virol 89:1925–1931. doi:10.1128/JVI.02262-14.

Editor: M. J. Imperiale

Address correspondence to Jia Liu, jliu4@uams.edu.

Copyright © 2015, American Society for Microbiology. All Rights Reserved.

doi:10.1128/JVI.02262-14

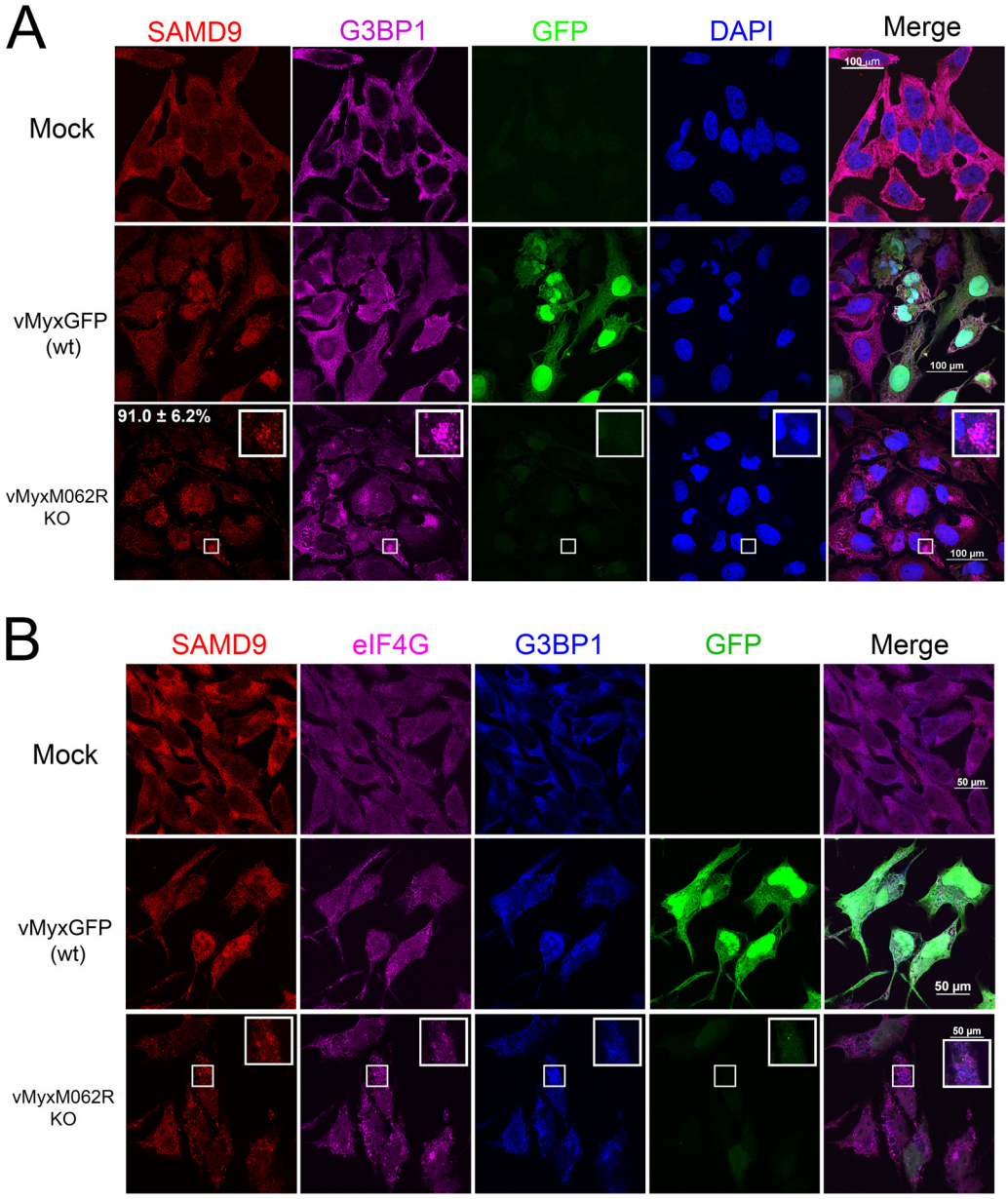

FIG 1 Infection by MYXV-M062R-null (vMyxM062RKO) leads to the formation of SAMD9 granules. (A) SAMD9 forms a granule structure during vMyxM062RKO infection. HeLa cells were mock treated or infected with wild-type MYXV [vMyxGFP (wt)] or vMyxM062RKO at a multiplicity of infection (MOI) of 10 for 18 h. Cells were fixed with 4% paraformaldehyde and permeabilized with cold methanol before they were incubated with primary antibodies (SAMD9 and G3BP1; Sigma-Aldrich and Santa Cruz Biotechnologies, respectively) and then secondary antibodies (Invitrogen). Samples were mounted for fluorescence microscopy (Nikon C2 confocal microscope). The scale bar represents a length of 100 μm. A total of 91.0% (±6.2% SD) of infected cells (GFP positive and/or viral factory positive) showed SAMD9 antiviral granules; within the viral factories, G3BP1 colocalizes with SAMD9 (the quantification was conducted from three independent experiments and four random views of image with 15 to 31 cells per view in each experiment). (B) SAMD9 granules colocalize with markers of stress granules (SGs). HeLa cells were mock treated or infected with wild-type MYXV or vMyxM062RKO viruses at a MOI of 10 for 18 h before immunofluorescence (IF) staining for SAMD9 (Alexa Fluor 594), G3BP1 (Alexa Fluor 350), and eIF4G (Alexa Fluor 647) was performed as described for panel A. Fluorescent images were captured with a Nikon C2 confocal microscope at 100× magnification. Scale bar, 50 μm.

were found to colocalize with the nucleated SAMD9 (Fig. 2A) at 5 h p.i. Our data show that SAMD9 granules stimulated by VACV-E3LKO-$_L$tdTr are indeed comparable to the previously reported antiviral granules (2). In addition, we show that double-stranded RNA (dsRNA) was also detected within the SAMD9 granule (Fig. 2B). We examined the phosphorylation status of eIF2α at these stages of the infections and found that the presence of SAMD9 granules was independent of eIF2α phosphorylation (Fig. 2C).

We next examined SAMD9 protein behavior under cellular stress conditions that either stimulated (sodium arsenate [SA] treatment at 1 mM for 1 h) or were independent of (desmethyl desamino pateamine A derivative [DMDA-PatA] treatment at 1 μM for 1 h) eIF2α phosphorylation (12, 13). When cells were stimulated with SA, an oxidative stress stimulus, along with other markers of SGs, SAMD9 nucleated into the SGs (Fig. 3). While DMDA-PatA targeted eIF4A to inhibit eukaryotic cap-dependent

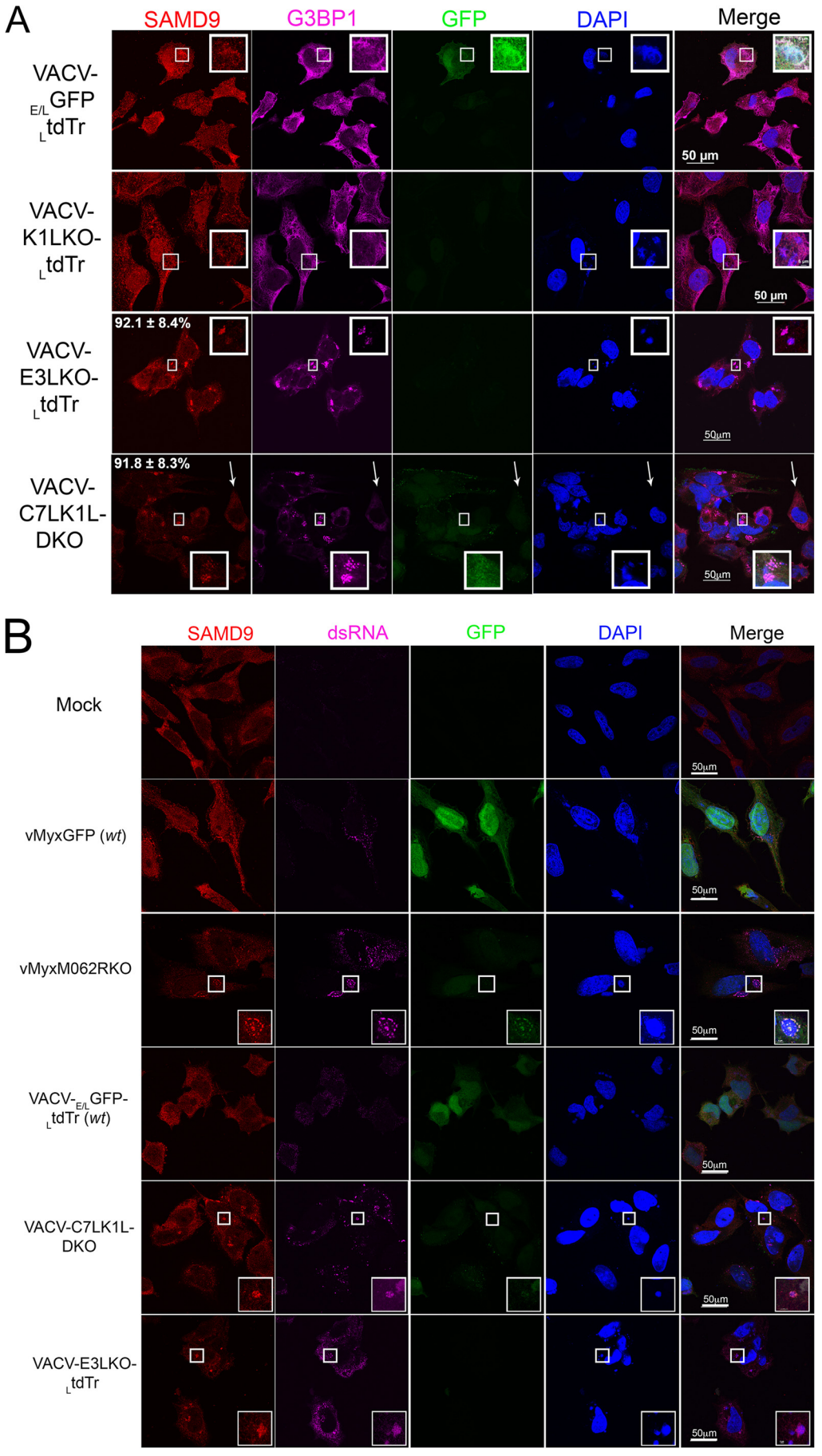
A
SAMD9
G3BP1
GFP
DAPI
Merge
VACV-E/LGFPLtdTr
VACV-K1LKO-LtdTr
VACV-E3LKO-LtdTr
VACV-C7LK1L-DKO
92.1 ± 8.4%
91.8 ± 8.3%
50 μm
50μm
B
SAMD9
dsRNA
GFP
DAPI
Merge
Mock
vMyxGFP (wt)
vMyxM062RKO
VACV-E/LGFP-LtdTr (wt)
VACV-C7LK1L-DKO
VACV-E3LKO-LtdTr
50μm

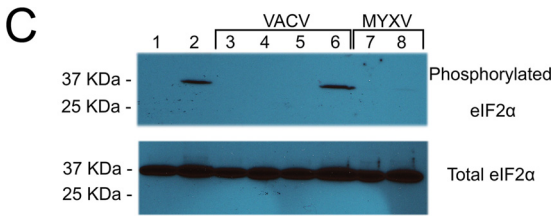

FIG 2 Abortive infection by E3L knockout VACV (VACV-E3LKO-$_L$tdTr) or C7LK1L double-knockout VACV (VACV-C7LK1L-DKO) stimulates SAMD9 granule formation. (A) SAMD9 antiviral granules form after VACV-E3LKO-$_L$tdTr (92.1% ± 8.4% SD) or VACV-C7LK1L-DKO (91.8% ± 8.3% SD) infection; meanwhile, G3BP1 colocalizes with SAMD9 in the viral factories. Wild-type or knockout VACV infection was conducted at a MOI of 5 for 5 h p.i. on HeLa cells before cells were fixed and permeabilized for IF staining of SAMD9 (Alexa Fluor 594) and G3BP1 (Alexa Fluor 647). Nuclei and viral factories were stained with DAPI (4′,6-diamidino-2-phenylindole). Low-level of tdTr expression driven by the late poxvirus promoter is not detectable at this time of the infection, and thus it does not interfere with the observation of Alexa Fluor 594. Fluorescent images were captured with a Nikon C2 confocal microscope. Quantification was conducted from the results of up to five independent experiments. The arrows point to an uninfected cell in the VACV-C7LK1L-DKO infection. Scale bar, 50 μm. (B) Double-stranded RNA can be detected within the SAMD9 granules. Infection by MYXV and VACV was conducted at 19 and 5 h p.i., respectively. After fixing and permeabilization, cells were probed with SAMD9, dsRNA (English and Scientific Consulting Kft.), and DAPI for IF. Fluorescence microscopic observation was performed as described for panel A. Scale bar, 50 μm. (C) The formation of SAMD9 antiviral granules by poxvirus infection is eIF2α phosphorylation independent. HeLa cells were infected with VACV (lane 3, VACV-$_{E/L}$GFP/$_L$tdTr; lane 4, VACV-K1LKO-$_L$tdTr; lane 5, VACV-C7LK1L-DKO; lane 6, VACV-E3LKO-$_L$tdTr) for 5 h at a MOI of 5 or with MYXV (lane 7, vMyxM062RKO; lane 8, vMyxGFP) for 19 h before they were harvested for Western blotting. As controls, cells were either mock treated (lane 1) or treated with sodium arsenate (SA) (1 mM) for 1 h (lane 2). Total proteins of 20 μg were separated using 12% SDS-PAGE before they were transferred to a polyvinylidene difluoride (PVDF) membrane for probing with phosphorylated eIF2α (Cell Signaling) and later with total eIF2α (Cell Signaling).

translation in an eIF2α phosphorylation-independent manner, SAMD9 was still recruited into the SGs (Fig. 3).

Thus, combining these findings, we conclude that SAMD9 is a stress response element that can respond to both viral stimuli (antiviral granules) and environmental stimuli (SGs) in both eIF2α-dependent and -independent manners.

Because MYXV-M062 was shown previously to functionally replace VACV-C7 in a VACV-C7LK1L-double-knockout background (8), we hypothesized that SAMD9 may be one of targets of the C7L superfamily. We engineered SAMD9 knockdown cell lines in both HeLa and A549 cells (ATCC CCL-185) (Fig. 4B and C) to examine the role of SAMD9 in antiviral granule formation. Although SAMD9 participated in antiviral granule formation along with hallmark factors of the SGs such as G3BP1 (Fig. 1 and 3), we would like to investigate whether SAMD9 plays a crucial role in organizing this antiviral structure.

Knocking down SAMD9 led to loss of the antiviral granule formation that would have been stimulated by either MYXV-M062R-null or VACV-C7LK1L-DKO infection, as G3BP1 was no longer able to nucleate (Fig. 4A). However, VACV-E3LKO-$_L$tdTr infection still led to G3BP1 granule formation (Fig. 4A) under the SAMD9 knockdown conditions. This suggests very different modes of organization of these antiviral granules. In SAMD9 knockdown cells, MYXV-M062R-null infection showed significant accumulation of viral GFP expression compared with infection in parental cells or control cells stably expressing the scramble short hairpin RNA (shRNA). Similar phenomena were also observed in VACV-C7LK1L-DKO infections, suggesting that knocking down SAMD9 expression lifted the block against the progression of viral gene expression. Viral replication by either MYXV-M062R-null or VACV-C7LK1L-DKO was rescued by SAMD9 knockdown (Fig. 4B and C).

There were, however, some differences between the SAMD9 antiviral granules induced by MYXV and those induced by VACV:

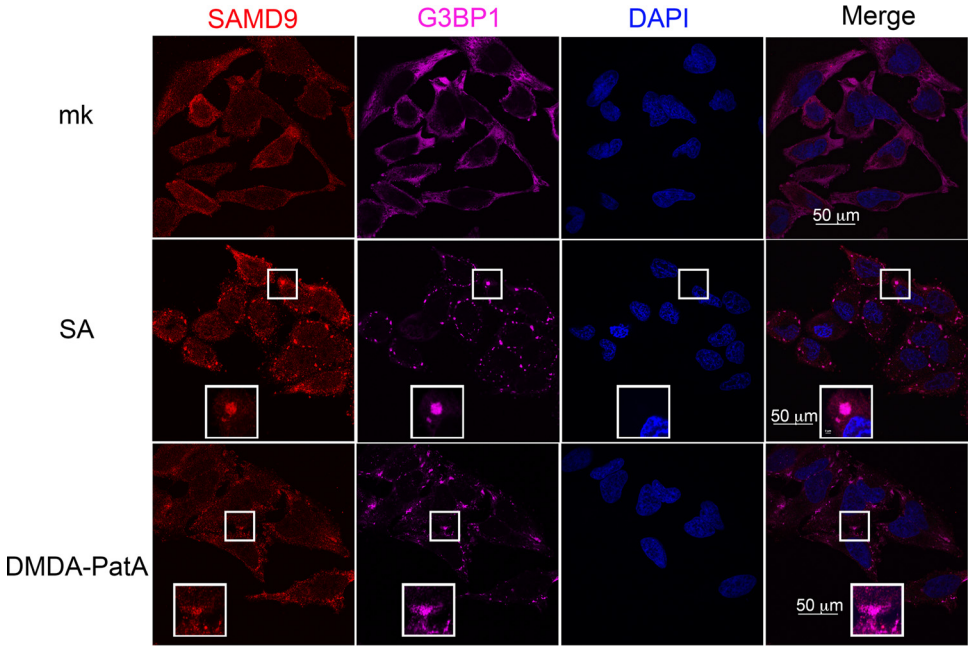

FIG 3 SAMD9 is a stress-responding element that participates in stress granule formation. HeLa cells are treated with sodium arsenate (SA) (1 mM) or DMDA-Pat A (1 μM) for 1 h before IF staining of SAMD9, G3BP1, and nuclei as described for Fig. 1 and 2. mk, mock treatment.

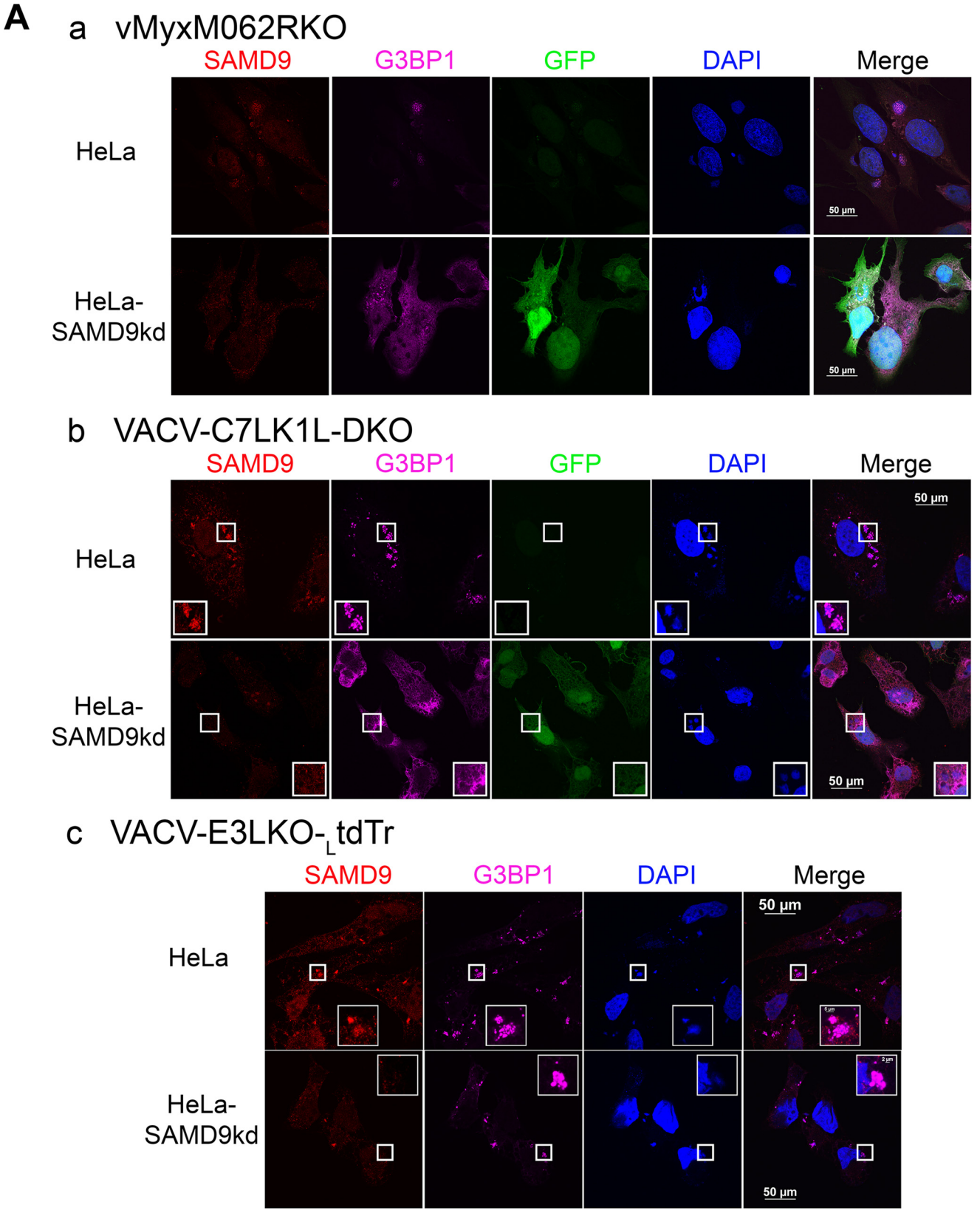
A
a vMyxM062RKO
SAMD9
G3BP1
GFP
DAPI
Merge
HeLa
HeLa-SAMD9kd
50 μm
b VACV-C7LK1L-DKO
SAMD9
G3BP1
GFP
DAPI
Merge
HeLa
HeLa-SAMD9kd
50 μm
c VACV-E3LKO-$_L$tdTr
SAMD9
G3BP1
DAPI
Merge
HeLa
HeLa-SAMD9kd
50 μm

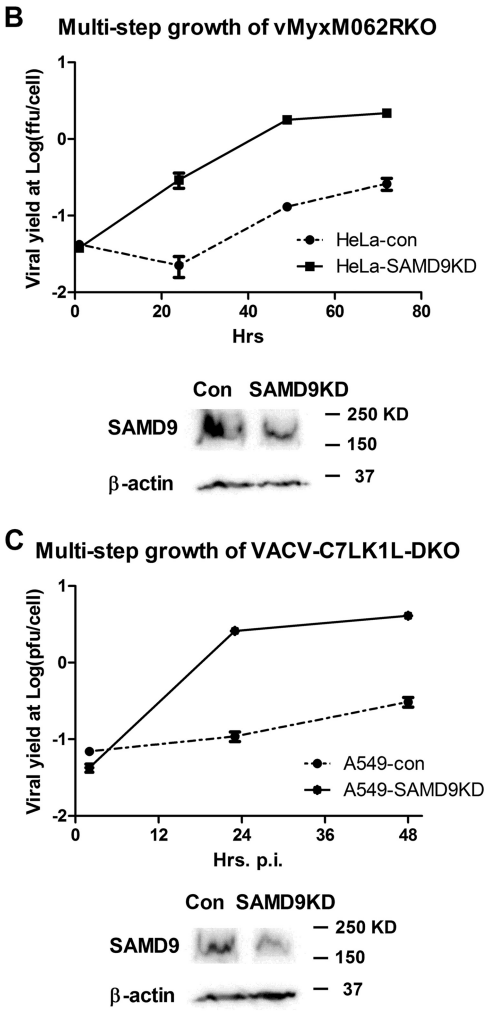

FIG 4 Knocking down SAMD9 rescues MYXV-M062R-null (vMyxM062RKO) and C7LK1L double-knockout VACV (VACV-C7LK1L-DKO) by disengaging the antiviral granule formation. (A) SAMD9 is responsible for the antiviral granule formation stimulated by either vMyxM062RKO (a) or VACV-C7LK1L-DKO (b) but not for the antiviral granule formation stimulated by E3L-knockout VACV (VACV-E3LKO-$_L$tdTr) (c). Antiviral granule formation was investigated at 19 h p.i. for vMyxM062RKO and at 5 h p.i. for VACV infection of normal HeLa cells or SAMD9 knockdown (SAMD9KD) at a MOI of 10 and a MOI of 5, respectively. After IF staining of SAMD9, G3BP1, and nuclei, images were captured with a Nikon c2 confocal microscope. Scale bar, 50 μm. (B) Knocking down SAMD9 expression rescues M062R-null MYXV replication. HeLa cells stably expressing shRNAs targeting SAMD9 (SAMD9KD) showed significantly reduced SAMD9 protein levels compared with control HeLa cells (con). A total protein of 40 μg was separated on SDS-PAGE for Western blotting against SAMD9 and β-actin. Multiple-step growth curve analysis of MYXV-M062R-null was conducted on control HeLa (con) or SAMD9 knockdown (SAMD9KD) HeLa cells. Duplicate of infection at each time point per virus was conducted. Titration was performed on BSC40 cells in triplicate at each dilution. The growth curve shown is one view representative of the results of two independent experiments. ffu, focus-forming units. (C) Knocking down SAMD9 expression rescues viral replication of VACV-C7LK1L-DKO. A549 cells stably expressing control shRNA (A549-con) or shRNAs targeting SAMD9 (A549-SAMD9KD) were engineered by infecting cells with lentivirus containing corresponding shRNAs. Western blot analysis was conducted with a total protein of 40 μg from either A549-con or A549-SAMD9KD by probing against SAMD9 and β-actin. The experiment designed to construct the multiple-step growth curve of VACV-C7LK1L-DKO was performed by infecting control or knockdown cells at a low MOI of 0.1 followed by harvesting at different time points. At each time point, samples from triplicate infections were collected for titration on BSC40 cells. The growth curve shown is a view representative of the results of two independent experiments.

SAMD9 granule formation was visualized at much later times in MYXV-M062R-null infection (18 h p.i.) than in VACV-C7LK1L-DKO infection (5 h p.i.). Note that late gene expression of MYXV can be detected at 8 h p.i. (1), while that of VACV can be detected by 6 h p.i. (14, 15). Furthermore, MYXV antagonizes SAMD9 through sequestration and redistribution by M062 direct interaction; however, how C7 or K1 functionally antagonizes SAMD9 during VACV infection remains to be investigated.

Knocking down SAMD9 at this moderate level (Fig. 4B and C) had no significant effect on improving wild-type VACV or MYXV replication. In addition, this moderate knockdown of SAMD9 in either HeLa or A549 did not jeopardize the cellular ability to form SGs as indicated by G3BP1 staining after SA or DMDA-PatA treatment (data not shown).

Concentrated dsRNA associated with abortive poxvirus infection was detected within SAMD9 antiviral granules, caused by VACV-E3LKO-$_L$tdTr, VACV-C7LK1L-DKO, or MYXV-M062R-null infection. However, only VACV-E3LKO-$_L$tdTr infection stimulated the phosphorylation of eIF2α at the time of antiviral granule formation (Fig. 2C). Vaccinia virus E3 binds to dsRNA, thus efficiently preventing the activation of the dsRNA-dependent protein kinase (PKR) (16, 17), which explains the eIF2α phosphorylation through PKR seen during E3LKO infection. However, because eIF2α phosphorylation was not detected at the time of antiviral granule formation by vMyxM062RKO or VACV-C7LK1L-DKO infection, we propose that there is likely a second mechanism that drives the formation of this antiviral structure. This correlates with the fact that SAMD9 knockdown rescues only the abortive infection by VACV-C7LK1L-DKO and vMyxM062RKO but not that by VACV-E3LKO-$_L$tdTr. Importantly, SAMD9 knockdown leads to the inability to form the antiviral granules only in VACV-C7LK1L-DKO-infected and vMyxM062RKO-infected cells. Thus, we concluded that at least two mechanisms are employed to organize the formation of these antiviral structures: one is eIF2α phosphorylation dependent, and the other is SAMD9 dependent.

ACKNOWLEDGMENTS

We thank J. Liem for assistance with software applications. We thank D. Romo (Texas A&M University) and his laboratory staff (J. Li and K. Hull) for supplying the DMDA-PatA.

This work was supported in part by NIH grant K22-A99184, grant P20-GM103625, and a startup fund by University of Arkansas for Medical Sciences (UAMS) provided to J. Liu. This work was also supported in part by grant R01-AI080607 to G. McFadden.

REFERENCES

1. **Liu J, Wennier S, Zhang L, McFadden G.** 2011. M062 is a host range factor essential for myxoma virus pathogenesis and functions as an antagonist of host SAMD9 in human cells. J Virol **85:**3270–3282. http://dx.doi.org/10.1128/JVI.02243-10.
2. **Simpson-Holley M, Kedersha N, Dower K, Rubins KH, Anderson P, Hensley LE, Connor JH.** 2011. Formation of antiviral cytoplasmic granules during orthopoxvirus infection. J Virol **85:**1581–1593. http://dx.doi.org/10.1128/JVI.02247-10.
3. **Tourrière H, Chebli K, Zekri L, Courselaud B, Blanchard JM, Bertrand E, Tazi J.** 2003. The RasGAP-associated endoribonuclease G3BP assembles stress granules. J Cell Biol **160:**823–831. http://dx.doi.org/10.1083/jcb.200212128.
4. **Kedersha NL, Gupta M, Li W, Miller I, Anderson P.** 1999. RNA-binding proteins TIA-1 and TIAR link the phosphorylation of eIF-2 alpha to the assembly of mammalian stress granules. J Cell Biol **147:**1431–1442. http://dx.doi.org/10.1083/jcb.147.7.1431.

5. **Wehner KA, Schutz S, Sarnow P.** 2010. OGFOD1, a novel modulator of eukaryotic translation initiation factor 2alpha phosphorylation and the cellular response to stress. Mol Cell Biol **30:**2006–2016. http://dx.doi.org/10.1128/MCB.01350-09.
6. **Kedersha N, Chen S, Gilks N, Li W, Miller IJ, Stahl J, Anderson P.** 2002. Evidence that ternary complex (eIF2-GTP-tRNA(i) (Met))-deficient preinitiation complexes are core constituents of mammalian stress granules. Mol Biol Cell **13:**195–210. http://dx.doi.org/10.1091/mbc.01-05-0221.
7. **Liu J, Rothenburg S, McFadden G.** 2012. The poxvirus C7L host range factor superfamily. Curr Opin Virol **2:**764–772. http://dx.doi.org/10.1016/j.coviro.2012.09.012.
8. **Meng X, Chao J, Xiang Y.** 2008. Identification from diverse mammalian poxviruses of host-range regulatory genes functioning equivalently to vaccinia virus C7L. Virology **372:**372–383. http://dx.doi.org/10.1016/j.virol.2007.10.023.
9. **Bartee E, Mohamed MR, Lopez MC, Baker HV, McFadden G.** 2009. The addition of tumor necrosis factor plus beta interferon induces a novel synergistic antiviral state against poxviruses in primary human fibroblasts. J Virol **83:**498–511. http://dx.doi.org/10.1128/JVI.01376-08.
10. **Meng X, Jiang C, Arsenio J, Dick K, Cao J, Xiang Y.** 2009. Vaccinia virus K1L and C7L inhibit antiviral activities induced by type I interferons. J Virol **83:**10627–10636. http://dx.doi.org/10.1128/JVI.01260-09.
11. **Villa NY, Bartee E, Mohamed MR, Rahman MM, Barrett JW, McFadden G.** 2010. Myxoma and vaccinia viruses exploit different mechanisms to enter and infect human cancer cells. Virology **401:**266–279. http://dx.doi.org/10.1016/j.virol.2010.02.027.
12. **Kuznetsov G, Xu Q, Rudolph-Owen L, Tendyke K, Liu J, Towle M, Zhao N, Marsh J, Agoulnik S, Twine N, Parent L, Chen Z, Shie JL, Jiang Y, Zhang H, Du H, Boivin R, Wang Y, Romo D, Littlefield BA.** 2009. Potent in vitro and in vivo anticancer activities of des-methyl, des-amino pateamine A, a synthetic analogue of marine natural product pateamine A. Mol Cancer Ther **8:**1250–1260. http://dx.doi.org/10.1158/1535-7163.MCT-08-1026.
13. **Low WK, Li J, Zhu M, Kommaraju SS, Shah-Mittal J, Hull K, Liu JO, Romo D.** 2014. Second-generation derivatives of the eukaryotic translation initiation inhibitor pateamine A targeting eIF4A as potential anticancer agents. Bioorg Med Chem **22:**116–125. http://dx.doi.org/10.1016/j.bmc.2013.11.046.
14. **Backes S, Sperling KM, Zwilling J, Gasteiger G, Ludwig H, Kremmer E, Schwantes A, Staib C, Sutter G.** 2010. Viral host-range factor C7 or K1 is essential for modified vaccinia virus Ankara late gene expression in human and murine cells, irrespective of their capacity to inhibit protein kinase R-mediated phosphorylation of eukaryotic translation initiation factor 2alpha. J Gen Virol **91:**470–482. http://dx.doi.org/10.1099/vir.0.015347-0.
15. **Ramsey-Ewing AL, Moss B.** 1996. Complementation of a vaccinia virus host-range K1L gene deletion by the nonhomologous CP77 gene. Virology **222:**75–86. http://dx.doi.org/10.1006/viro.1996.0399.
16. **Langland JO, Jacobs BL.** 2004. Inhibition of PKR by vaccinia virus: role of the N- and C-terminal domains of E3L. Virology **324:**419–429. http://dx.doi.org/10.1016/j.virol.2004.03.012.
17. **Zhang P, Jacobs BL, Samuel CE.** 2008. Loss of protein kinase PKR expression in human HeLa cells complements the vaccinia virus E3L deletion mutant phenotype by restoration of viral protein synthesis. J Virol **82:**840–848. http://dx.doi.org/10.1128/JVI.01891-07.